ADVANCED OPTICAL MATERIALS

Supporting Information

Effectively Transparent Front Contacts for Optoelectronic Devices

Rebecca Saive, Aleca M. Borsuk, Hal S. Emmer, Colton R. Bukowsky, John V. Lloyd, Sisir Yalamanchili, and Harry A. Atwater*

Supplemental: Effectively transparent front contacts for optoelectronic devices

Rebecca Saive[1], Aleca M. Borsuk[1], Hal S. Emmer[1], Colton R. Bukowsky[1], John V. Lloyd[1], Sisir Yalamanchili[1], and Harry A. Atwater[1*]

[1] Department of Applied Physics and Material Science, California Institute of Technology, Pasadena, CA 91125, USA

## S1: Optical simulations and measurements of the wavelength and angle dependence
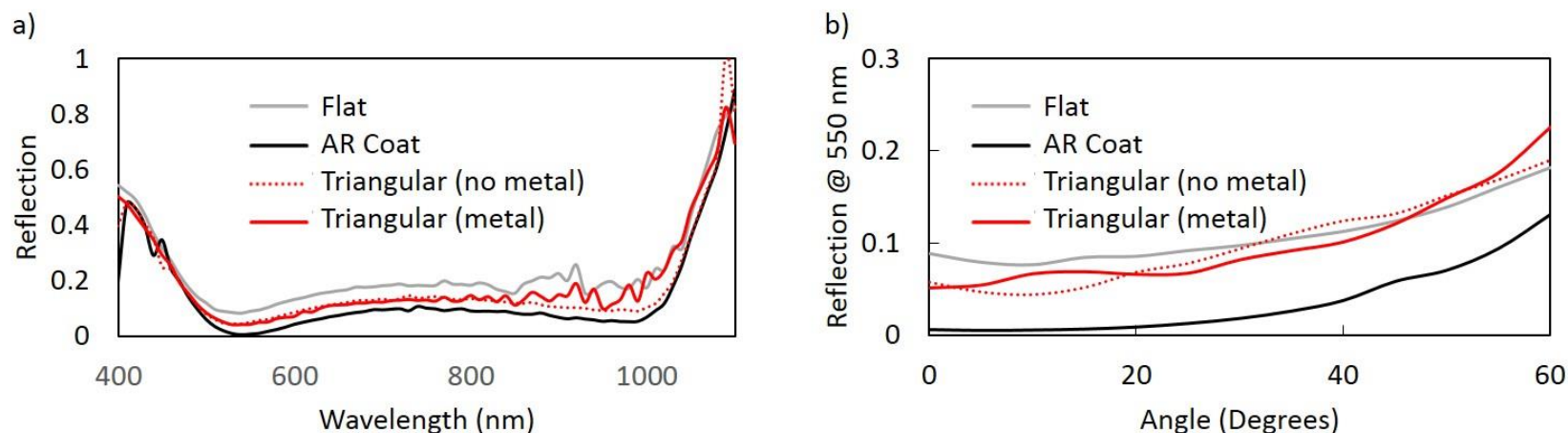
Figure S1.1: a) Measured wavelength dependent reflection and b) angle dependent reflection of areas on the solar cell with flat lines, triangular cross-section lines and only the antireflection coating. Angle and wavelength dependent reflection measurements were performed in a spectrophotometer equipped with an integrating sphere. The spectrophotometer instrument uses chopped monochromated light from a supercontinuum laser and a silicon photodiode detector, as described elsewhere (M.D. Kelzenberg, PhD thesis, 2010). The axis of angular rotation was aligned parallel to the contact finger lines or triangular contacts (compare angle α in Fig. S1.2). In contrast to the spatially resolved photocurrent measurements presented in the main manuscript in Fig. 2 the illumination spot size used in these measurements is large (~ 200 µm), and averages over regions with good fidelity in the fabricated triangular cross-section contact structure, along with regions containing imperfections.
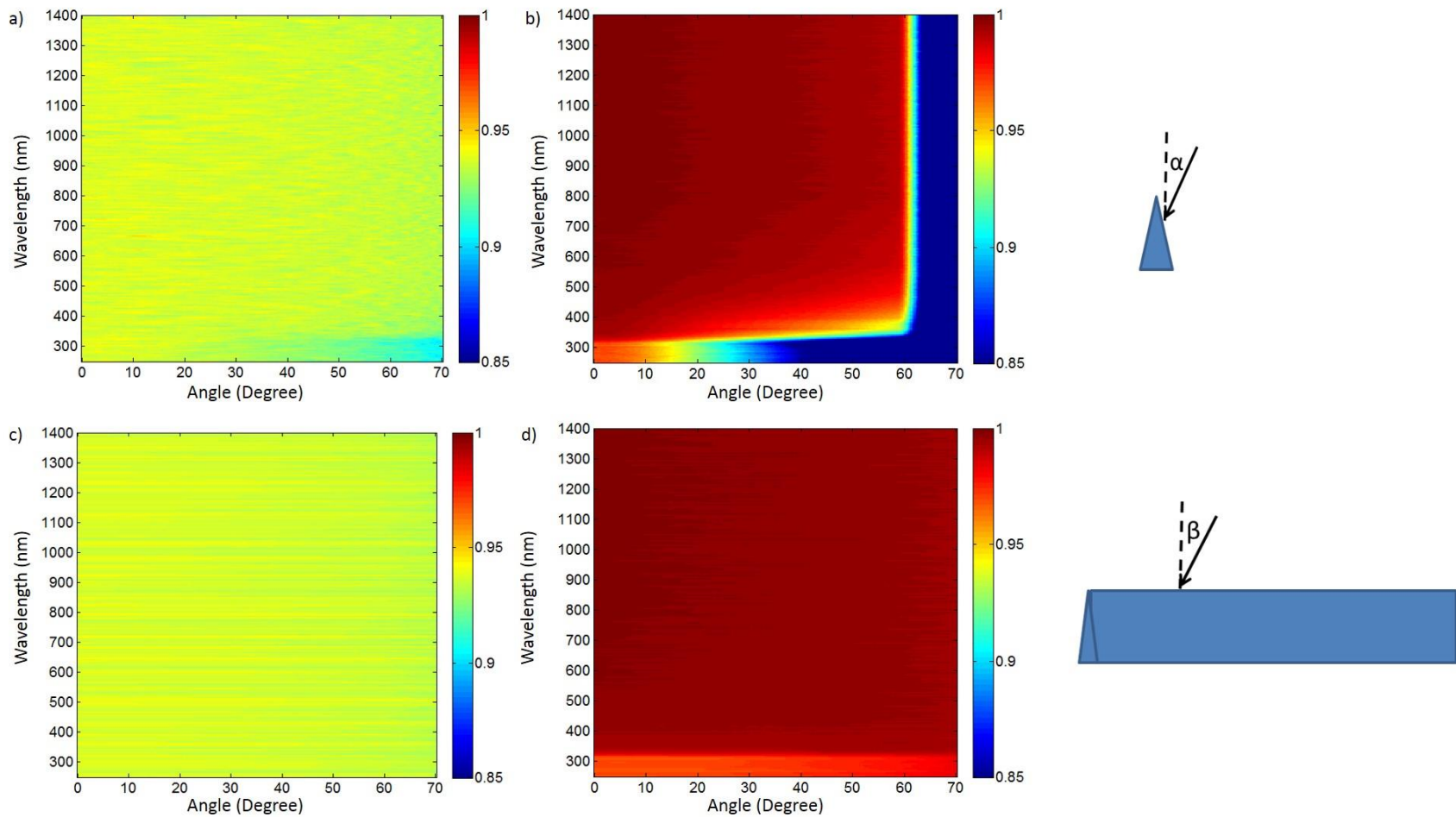
Figure S1.2: Ray optical (Lighttools) simulation of the wavelength and angle dependence of the transmission through a grid of free-standing a), c) flat silver lines and b), d) triangular cross-section silver lines. In a) and b) the angle was varied perpendicular to the line (angle α on the right side), in c) and d) the angle was varied parallel to the contact lines (angle β on the right side). Decreased transparency in the short wavelength regime can be attributed to losses in the silver.

## S2 Optical simulation of triangular cross-section line patterns with different periods
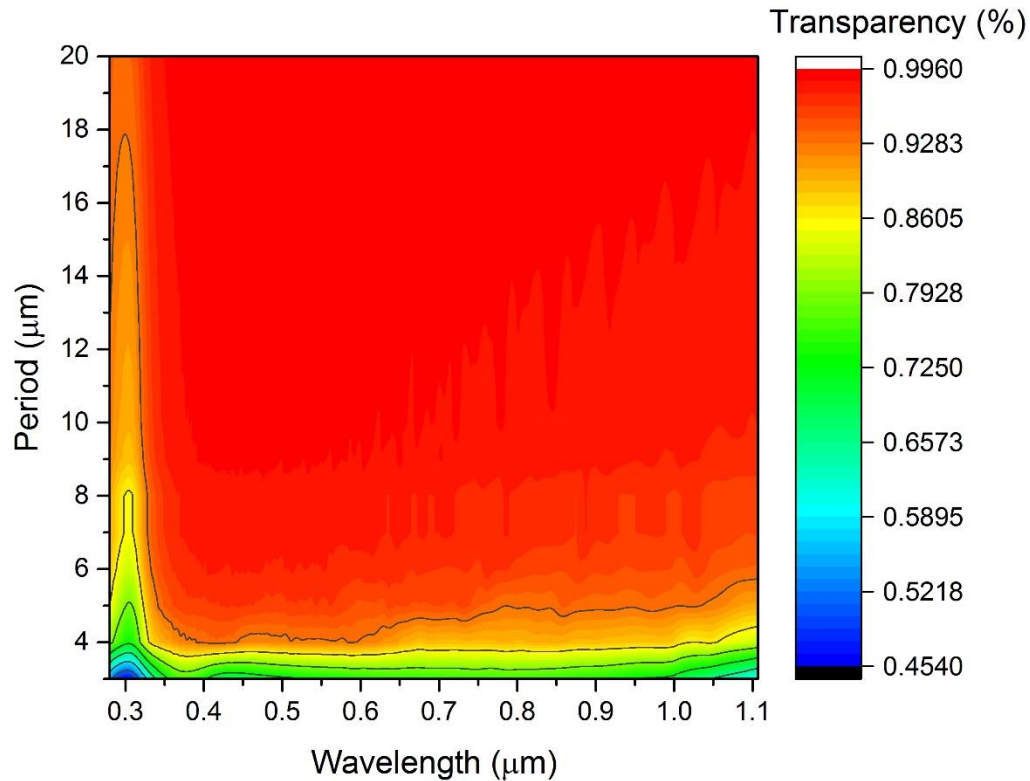

Figure S2: Simulation of the transparency of free-standing, solid silver triangular cross-section lines depending on the wavelength and on the period of the line pattern. The simulation was performed by two-dimensional rigorous coupled wave analysis (RCWA) using RSofts's DiffractMOD in order to account for wave optical effects occurring particularly for smaller periods. Periods between 3 µm and 20 µm and wavelengths between 280 nm and 1107 nm were simulated. The triangular lines were 2.5 µm wide and 7.0 µm high. Thus, e.g. a period of 6.0 µm corresponds to a gap of 3.5 µm. It can be seen that the transparency remains almost 100 % for periods down to around 5 µm. Decreased transparency in the short wavelength regime can be attributed to losses in the silver.

S3: Comparison of different photonic approaches to improved front contact transparency

Title	Authors	Paper	Scheme	Transparency	Equivalent current*	Sheet resistance
Effectively transparent front contacts for optoelectronic devices	Rebecca Saive, Aleca M. Borsuk, Hal S. Emmer, Colton R. Bukowsky, John V. Lloyd, Sisir Yalamanchili, and Harry A. Atwater	This paper		99.9 %	41.21 mA/cm^2	4.8 Ω/sq
24.7% Record Efficiency HIT Solar Cell on Thin Silicon Wafer	Mikio Taguchi, Ayumu Yano, Satoshi Tohoda, Kenta Matsuyama, Yuya Nakamura, Takeshi Nishiwaki, Kazunori Fujita, and Eiji Maruyama	IEEE Journal of Photovoltaics 4, 96-99 (2014)		~ 96.6 %[1] (only grid fingers, deduced from geometry and current)	39.5 mA/cm^2	~ 5 Ω/sq[1]
Hybrid Metal–Semiconductor Nanostructure for Ultrahigh Optical Absorption and Low Electrical Resistance at Optoelectronic Interfaces	Vijay K. Narasimhan, Thomas M. Hymel, Ruby A. Lai, and Yi Cui	*ACS nano* **9**, 10590-10597 (2015)		97 % absorption, with 4.2 % parasitic absorption within metal → 92.8 % transmission	38.40 mA/cm^2	Below 20 Ω/sq
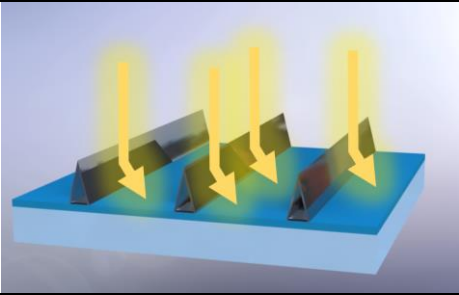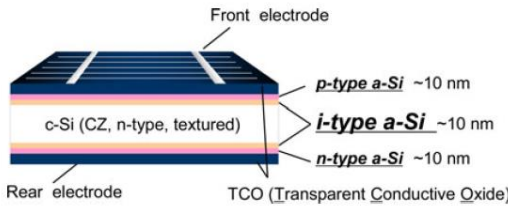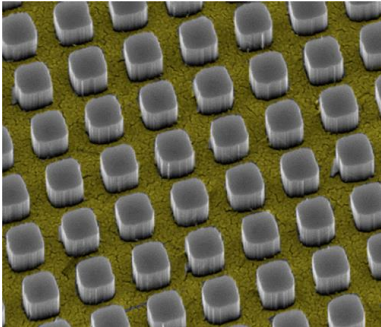
Cloaked contact grids on solar cells by coordinate transformations: designs and prototypes	Martin F. Schumann, Samuel Wiesendanger, Jan Christoph Goldschmidt, Benedikt Bläsi, Karsten Bittkau, Ulrich W. Paetzold, Alexander Sprafke, Ralf B. Wehrspohn, Carsten Rockstuhl, and Martin Wegener	*Optica* **2**, 850-853 (2015)		Transparency not explicitly reported.	---	Not reported but this geometry should allow for low sheet resistance.
Catoptric electrodes: transparent metal electrodes using shaped surfaces	Pieter G. Kik	*Optics letters* **39**, 5114-5117 (2014)		84 % (Simulation)	34.68 mA/cm^2	Not reported but this geometry should allow for low sheet resistance.
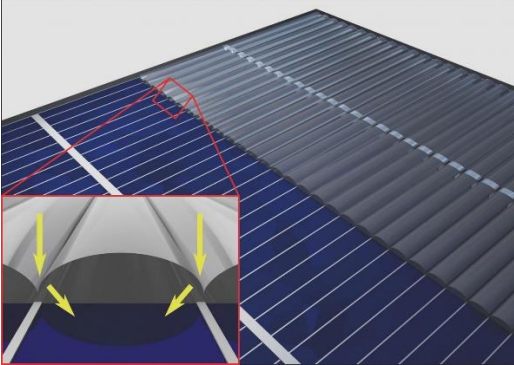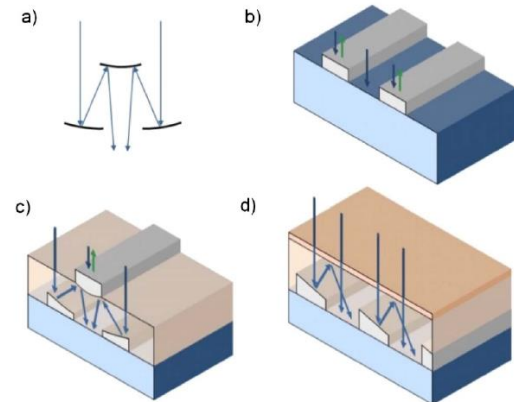
| Transparent metallic fractal electrodes for semiconductor devices	Farzaneh Afshinmanesh, Alberto G. Curto, Kaveh M. Milaninia, Niek F. van Hulst, and Mark L. Brongersma	*Nano letters* **14**, 5068-5074 (2014)		No average transparency reported.	---	No sheet resistance reported.
Performance enhancement of metal nanowire transparent conducting electrodes by mesoscale metal wires	Po-Chun Hsu, Shuang Wang, Hui Wu, Vijay K. Narasimhan, Desheng Kong Hye Ryoung Lee and Yi Cui	*Nature communications* **4** (2013)		92 %	38.10 mA/cm^2	0.36 Ω/sq
Transparent Conducting Silver Nanowire Networks	Jorik van de Groep, Pierpaolo Spinelli, and Albert Polman	*Nano Letters* **12**, 3138-3144 (2012)		91 %	37.67 mA/cm^2	6.5 Ω/sq
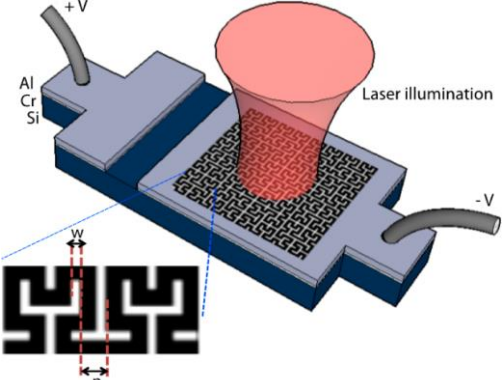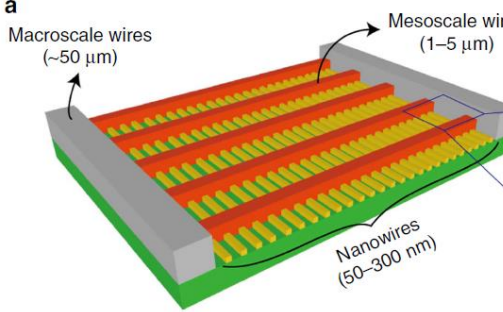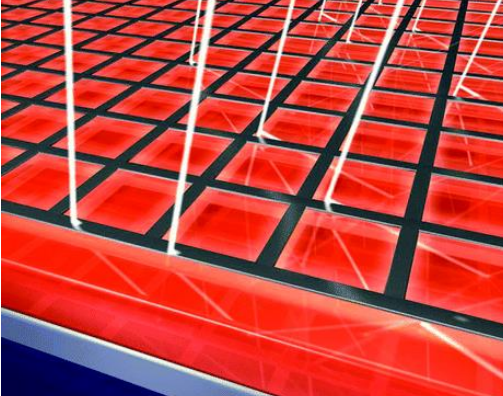
* The equivalent circuit is calculated at the example of the 24.7 % efficiency Panasonic HIT cell (*IEEE Journal of Photovoltaics* **4**, 96-99 (2014)). The grid fingers are replaced by using a contact structure with the reported transparency, the busbars are kept the same. Furthermore, a current of 1.21 mA/cm^2 is subtracted in order to account for parasitic absorption within the amorphous silicon.

For our contact structure we also performed a realistic ray tracing simulation that takes the front texture of silicon in real solar cells and losses in the amorphous silicon into account. Note, that it is not clear for all structures reported here how integration with structured silicon would be achieved.

[1] These values are not explicitly given in the paper but deduced from the optical and electrical properties by comparison with similar solar cells.

S4: Additional spatially resolved laser beam induced photocurrent measurement

The left figure shows a spatially resolved laser beam induced photocurrent measurement of an area on the very same solar cell used for the measurement in Fig 2. In this area an approximately 100 nm silver layer covers the flat lines as a result from the angular evaporation. The silver was evaporated from the right side so that right of the line there is a silver hill while left of the line is only little or no silver. From the profile shown on the right side, it can be seen that there is a non-negligible photocurrent induced between the lines although this area was covered with around 100 nm of silver. The signal goes down to zero at the position of the silver hills showing that this is not a measurement artifact but that 100 nm of silver transmit a significant amount of light.
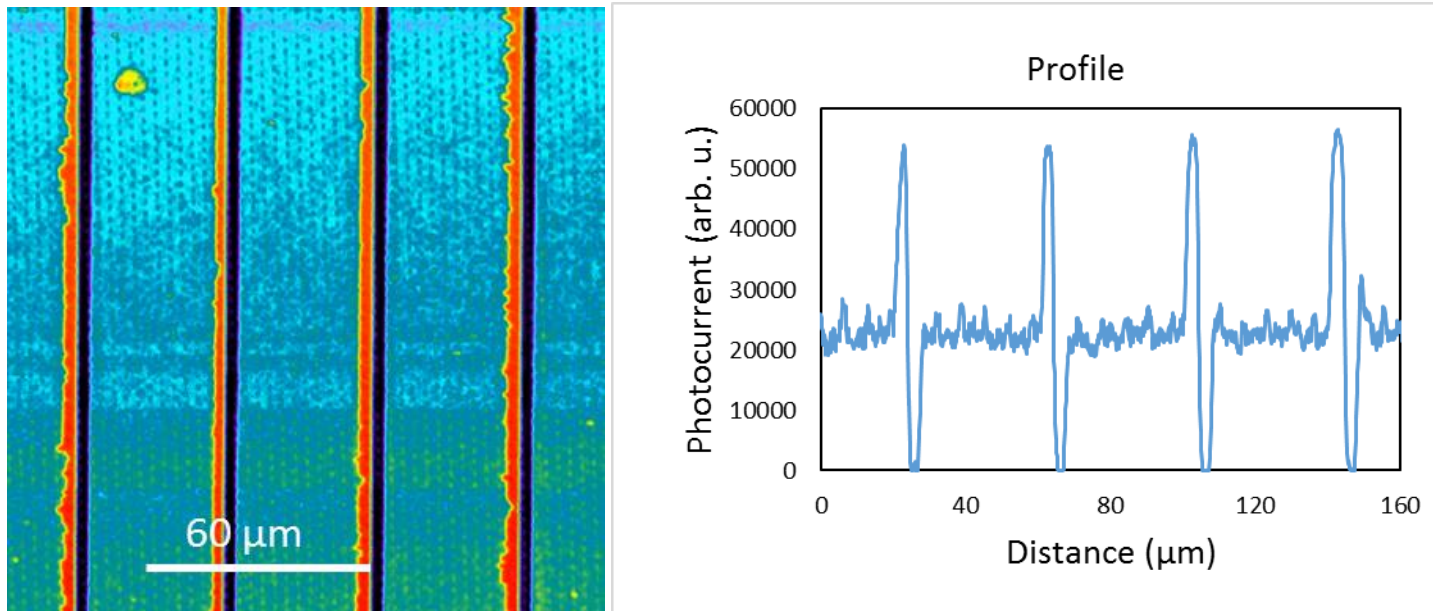
S5: Electrical properties of the line grid

Transport to metal finger   Transport within metal finger

$$P_{loss} = I^2 R = \frac{1}{2} \int_0^{w/2} j^2(x,y) x^2 L^2 \rho_\square \frac{dx}{L} + \int_0^L j^2(x,y) w^2 y^2 \, \rho_{Ag} \frac{dy}{t_{Ag} w_{Ag}}$$

Charge generation profile

$$\rightarrow P_{loss} = j^2 L \rho_\square \frac{w^3}{24} + j^2 w^2 \, \rho_{Ag} \frac{L^3}{3 t_{Ag} w_{Ag}} = I^2 \rho_\square \frac{w}{24L} + I^2 \, \rho_{Ag} \frac{L}{3 t_{Ag} w_{Ag}}$$

(with $j^2(x,y) = const$)

Assuming a length of 1 cm with the device geometry shown we obtain:

$$\boxed{R_s = P_{loss}/I^2 = 1.0 \, \Omega cm^2}$$

with $\rho_{\square(a-Si)} = 400 \; k\Omega/sq^*$ and $\rho_{Ag} = 1.6 \cdot 10^{-6} \Omega cm$.

(With $j = 40 \; mA/cm^2$ the power loss would amount to $1.6 \; mW/cm^2$)
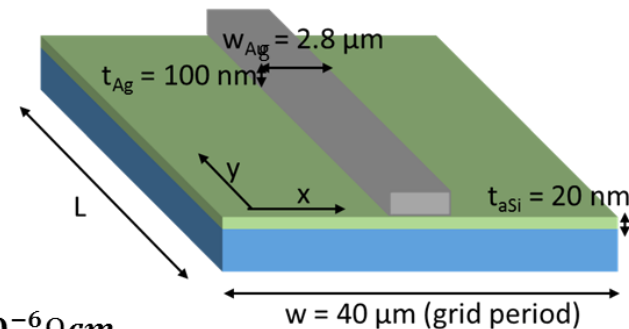
*Filipic et al.: JOURNAL OF APPLIED PHYSICS 114, 074504 (2013)

$w_{Ag} = 2.8$ µm
$t_{Ag} = 100$ nm
$t_{aSi} = 20$ nm
$w = 40$ µm (grid period)